

# Comparison of Near Threshold Fatigue Crack Growth Data by Kmax-constant Method with the Post-Construction Codes

メタデータ	言語: English 出版者: 公開日: 2007-09-25 キーワード (Ja): キーワード (En): 作成者: MESHII, Toshiyuki, WATANABE, Katsuhiko メールアドレス: 所属:
URL	<a href="http://hdl.handle.net/10098/1128">http://hdl.handle.net/10098/1128</a>

T. Meshii, et al., Nuclear Engineering and Design, Vol. 220, No. 3, pp. 285-292 (2003. 2).

**Comparison of Near Threshold Fatigue Crack Growth Data by  $K_{\max}$ -constant Method  
with the Post-Construction Codes**

Toshiyuki MESHII<sup>a</sup> and Katsuhiko WATANABE<sup>b</sup>

<sup>a</sup> Department of Mechanical Engineering, Fukui University, 3-9-1, Bunkyo, Fukui, 910-8507, Japan

Tel. & Fax. +81-776-27-8468, e-mail: meshii@mech.fukui-u.ac.jp

<sup>b</sup> 1<sup>st</sup> Division, Institute of Industrial Science, University of Tokyo, 4-6-1, Komaba, Meguro-ku, Tokyo 153-8505,

Japan

**ABSTRACT**

In this paper we obtain near threshold fatigue crack growth (FCG) data for several carbon steels and type 304 stainless steel by the  $K_{\max}$ -constant method. Since the FCG rate obtained by the  $K_{\max}$ -constant method is considered to give the upper limit of the FCG data obtained by the stress ratio-constant method, this data was compared with the FCG evaluation diagrams given in the ASME and JSME pressure vessel post-construction codes to ensure their validity. Though the FCG rate for carbon steel S55C was somewhat affected by the  $K_{\max}$  value, the results show that the obtained near threshold FCG data is close to the upper bound of the JSME code diagram, which is an extrapolation of the ASME FCG diagram to the near threshold region.

*KEY WORDS:* Fracture Mechanics, Fatigue Crack Growth, Threshold, Maximum Stress Intensity, Post-Construction Codes.

## 1. Introduction

Since the pioneering work of Paris and Erdogan (1963), the fatigue crack growth (FCG) rate  $da/dN$  under small scale yielding conditions has been described by the applied stress intensity range  $\Delta K$  for various materials. low FCG rates,  $da/dN - \Delta K$  curves in log-log scale generally become steep and appear to approach a vertical asymptote that corresponds to the FCG threshold. Tests near this threshold are time consuming in general, and as a result, data in this region are not always easy to obtain. So when the near threshold FCG rate data for a specific material is not given, there are instances where the medium range FCG rate data for the material is linearly extrapolated to the near threshold range on the log-log scale (*linear extrapolation*). This extrapolation is a natural engineering approach because it is generally considered as being safe assuming that the FCG threshold exists. One example for this extrapolation is the FCG rate evaluation curve in the Japan Society of Mechanical Engineers' nuclear power plant post construction code (JSME code) (JSME, 2001). JSME code's FCG rate evaluation curve which covers  $da/dN \geq 1 \times 10^{-7}$  mm/cycle, is an extrapolation of the well-known ASME pressure vessel code Sec. XI (ASME, 1998) applicable for  $da/dN \geq 25.4 \times 10^{-7}$  mm/cycle ( $1 \times 10^{-7}$  in/cycle).

Recently Marci (1996) reported that the FCG threshold ceases to exist for a Ti-6Al-2Sn-4Zr-6Mo alloy under high maximum stress intensity  $K_{max}$ , though their  $K_{max}$ -constant FCG tests (Döker, 1981) were conducted under a  $\Delta K - a$  relationship specified in ASTM E-647

(1999) (Marci effect). In this case  $da/dN$  was greater than  $1 \times 10^{-5}$  mm/cycle, though the expected rate obtained by the *linear extrapolation* was as small as  $1 \times 10^{-8}$  mm/cycle. Lang et al.'s report (1998) should have encouraged code engineers (who are interested in the *linear extrapolation*) because the Marci effect was assumed as a result of a combination of corrosive environment and the specific material. On the other hand, Newman et al.'s (2000) near threshold FCG rate data for Al7050-T6 alloy raises some concerns over the *linear extrapolation*. Their data obtained by the  $K_{\max}$ -constant method showed on the one hand the validity of *linear extrapolation*, and on the other hand that the near threshold  $da/dN$  was increased by an increase in  $K_{\max}$  without a corrosive atmosphere. The mechanism for this phenomenon is not yet clear.

Considering the findings above, we decided to obtain near threshold  $da/dN$  data for various materials (not only those used for nuclear power plants). As a first step, we obtained  $da/dN$  data in the range of  $1 \times 10^{-7} \leq da/dN \leq 1 \times 10^{-5}$  mm/cycle for carbon steels (JIS S55C, HT60 and SS400) and type 304 stainless steel in a laboratory air environment. We selected the  $K_{\max}$ -constant method for the test, because the upper limit of  $da/dN$  data obtained by the stress ratio  $R$ -constant tests is said to be expected since closure free conditions are realized in this method (Hertzberg, 1992). The effects of  $K_{\max}$  on  $da/dN$  data were studied at the same time.

## **2. Test conditions and results**

### **2.1 Test conditions**

We made tests fundamentally in accordance with the  $\Delta K$ -decreasing threshold test procedure specified in ASTM E647 (ASTM, 1999) in association with a constant maximum stress intensity level  $K_{\max}$  (Döker, 1981). The testing system and dimensions of the CT test specimen are shown in Figs. 1 and 2, respectively. Chemical compositions and the mechanical properties of the tested materials are given in Tables 1 and 2, respectively.

The cyclic stress intensity range was varied according to the following relationship, as specified in ASTM E647 (ASTM, 1999):

$$\Delta K = \Delta K_0 e^{C(a-a_0)} \dots\dots\dots (1)$$

where  $a_0$  (= initial machine notch length 15 mm+ fatigue pre-cracking 3 mm = 18 mm) and  $a$  are initial and current values of the crack length respectively.  $\Delta K_0$  is the initial value of  $\Delta K$  set to a value 12 MPam<sup>1/2</sup> for all the materials and regardless of  $K_{\max}$ . This value of  $\Delta K_0$  was chosen to make  $\Delta K = 3$  MPam<sup>1/2</sup> at  $a = 20$ mm, considering the fact that the threshold  $\Delta K$  of various ferritic alloys are about 3 MPam<sup>1/2</sup>.  $C$  is the normalized  $K$ -gradient  $(d(\Delta K)/da)/\Delta K$  set to a value of  $C = -0.7$  mm<sup>-1</sup>, which is a deviation from the ASTM E647 specification  $C > -0.08$  mm<sup>-1</sup> based on the  $R$ -constant test method. This deviation is validated in the case of the  $K_{\max}$ -constant test method for a value of  $C$  as small as  $C = -1.2$  mm<sup>-1</sup>. This is based on work by Hertzberg et al. (1992), who explain that this is true because the crack tip plastic zone size is held constant for  $K_{\max}$ -constant tests.

For each material, tests were conducted for several values of  $K_{\max}$ , that were chosen to satisfy

the small scale yielding condition required in ASTM E647;  $K_{\max} < K_{\max 0} \equiv \sigma_{YS} (\pi (W - a)/4)^{1/2}$ , where  $\sigma_{YS}$  is the yield strength of the material. In concrete, S55C:  $K_{\max} = 50, 46, 42, 36, 18$  MPam<sup>1/2</sup> ( $K_{\max}/K_{\max 0} = 0.87, 0.80, 0.73, 0.63, 0.31$ ), HT60:  $K_{\max} = 80, 70, 50, 30$  MPam<sup>1/2</sup> ( $K_{\max}/K_{\max 0} = 1.00, 0.88, 0.63, 0.38$ ), SS400:  $K_{\max} = 42, 32, 18$  MPam<sup>1/2</sup> ( $K_{\max}/K_{\max 0} = 0.99, 0.76, 0.43$ ), SUS304:  $K_{\max} = 31, 25, 18$  MPam<sup>1/2</sup> ( $K_{\max}/K_{\max 0} = 0.90, 0.72, 0.52$ ).

## 2.2 Test results

Comparison of the planned and the measured  $\Delta K - a$  relationship for the case of SUS 304 under  $K_{\max} = 31$  MPam<sup>1/2</sup> is shown in Fig. 3. The maximum difference in  $\Delta K$  for the planned and measured was as small as 4.4% in Fig. 3 and was less than 5% for other tests. For all tests, closure free is confirmed by measuring back surface strain. The loading frequency was 30 Hz.

The  $da/dN$  data we obtained for HT60, SS400, SUS304 and S55C are summarized in Figs. 4 to 7, respectively. We measured the crack length with an optical micrometer with a resolution of 1/100 mm and evaluated  $da/dN$  by the incremental polynomial method given in ASTM E647. Since we plan to compare the  $da/dN$  data obtained with the FCG evaluation curves in the post-construction codes, we fundamentally obtained data in the range of  $1 \times 10^{-7} \leq da/dN \leq 1 \times 10^{-5}$  mm/cycle.

We see from Figs. 4 ~6 that though tests for HT60, SS400 and SUS304 were conducted for several  $K_{\max}$  satisfying  $W-a \geq (4/\pi)(K_{\max}/\sigma_{YS})^2$ , the  $da/dN$  data within the measured range showed little variance and a clear threshold  $\Delta K$  existed.

On the other hand, we see in Fig. 7 that the trend observed for the S55C was somewhat different from the other materials. Though the  $da/dN$  data shows little variance for  $da/dN > 10^{-6}$  mm/cycle, the  $da/dN$  seemed to increase according to the increase in  $K_{max}$  in the range of  $1 \times 10^{-7} \leq da/dN \leq 1 \times 10^{-6}$  mm/cycle, which is similar to what Newman et al. (2000) experienced.

The data we obtained were compared with the JSME code's FCG evaluation curve in Figs. 8 (carbon steel) and 9 (stainless steel). In these figures, there are different symbols for each material, but  $K_{max}$  test values for each material are not distinguished from one another. JSME code's FCG evaluation curve in the range  $1 \times 10^{-7} \leq da/dN \leq 25.4 \times 10^{-7}$  mm/cycle is a *linear extrapolation* of the ASME sec. XI's corresponding curve, which is specified in the range of  $da/dN \geq 25.4 \times 10^{-7}$  mm/cycle ( $1 \times 10^{-7}$  in/cycle). We see from these two figures that our data obtained by the  $K_{max}$ -constant method and in the range of  $1 \times 10^{-7} \leq da/dN \leq 1 \times 10^{-5}$  mm/cycle, were in the range of JSME code's two curves for  $R = 0$  and 0.9. This was true also for S55C, which was affected by the value of  $K_{max}$ . Thus we conclude that the *linear extrapolation* of the ASME sec. XI's FCG evaluation diagram in the range of  $da/dN \geq 1 \times 10^{-7}$  mm/cycle is valid for the tested materials.

### 3. Discussion

Of the materials we tested, only S55C showed any sign of Marci effect (Marci, 1996) that is an effect of  $K_{max}$  at the FCG threshold, although the effect was small. Since the current understanding of the Marci effect is associated with sustained-load cracking (Lang et al., 1998), we

compared fractographs from scanning electron microscopy corresponding to  $da/dN \approx 1 \times 10^{-5}$  mm/cycle ( $a = 18$  mm) and  $da/dN \approx 1 \times 10^{-7}$  mm/cycle at two test conditions of  $K_{\max} = 50$  and 18 MPam<sup>1/2</sup>. No apparent differences in fractography were found for these  $K_{\max}$ s. Fractographs for  $K_{\max} = 50$  MPam<sup>1/2</sup> are shown as Figs. 10 and 11, respectively.

We see from Fig. 10 that striation-like spacing in the tested  $da/dN$  region (in which Paris' law is applicable) does not necessarily coincide with the  $da/dN$  and that the spacing can be 100 times larger than the  $da/dN$ . These results do not contradict with the Davidson et al.'s overview report (1992). In the near threshold region, as shown in Fig.11, we could not find out corrosion pits, though the high  $K_{\max}$  affected  $da/dN$ . Thus we conclude that the way that the high  $K_{\max}$  affected  $da/dN$  for S55C is not associated with sustained-load cracking and is different from what Marci et al. reported for Ti-6Al-2Sn-4Zr-6Mo alloy.

When we think about the fact that the  $da/dN$  for S55C in the near threshold region did not exceed  $da/dN$  obtained by *linear extrapolation* for all  $K_{\max}$ s, this observation may be close to what Newman et al. (2000) reported for Al7050-T6 alloy by the  $K_{\max}$  test method. They pointed out that dimples tended to increase in the near threshold region when they increased  $K_{\max}$ . However, we did not observe any dimples as can be seen from Fig. 11. On the other hand, a river pattern was found in Fig. 11, though the area ratio for this pattern was small. In addition, this area ratio did not appear to change with the changes in the  $K_{\max}$  test conditions. At this time, we cannot completely explain the

mechanism for how  $K_{\max}$  affects  $da/dN$  and further study seems to be necessary on this point.

However, in an engineering sense, we conclude that *linear extrapolation* in a non-corrosive atmosphere is valid and on the safe side.

#### 4. Conclusions

In this paper we report on near threshold fatigue crack growth (FCG) data in  $1 \times 10^{-7} \leq da/dN \leq 1 \times 10^{-5}$  mm/cycle for carbon steels S55C, HT60 and SS400 and type 304 stainless steel by the  $K_{\max}$ -constant method. Since the FCG rate by the  $K_{\max}$ -constant method is considered to give the upper limit of the FCG data obtained by the stress ratio-constant method, the data we obtained were compared with the FCG evaluation diagrams given in the ASME and JSME pressure vessel post-construction codes to ensure their validity. Though the FCG rate for carbon steel S55C was somewhat affected by the  $K_{\max}$  value, our results show that the FCG data obtained near threshold is close to the upper bound of the JSME code diagram, which is an extrapolation of the ASME FCG diagram to the near threshold region. From this work we conclude that the linear extrapolation of  $da/dN$  data in the medium range FCG area to the near threshold area is valid.

#### References

ASME, 1995. Boiler and pressure vessel code section XI. ASME, New York, Appendix C.

T. Meshii, et al., Nuclear Engineering and Design, Vol. 220, No. 3, pp. 285-292 (2003. 2).

ASTM, 1999. 1999 Annual Book of ASTM Standards, Vol. 03-01, ASTM, West Conshohocken, pp. 577-613.

Davidson, D. L. and Lankford, J., 1992. Fatigue crack growth in metals and alloys: mechanisms and micromechanics. Int. Materials Reviews. 37, 45-76.

Döker, H., Bachmann, V. and Marci, G., 1981. A comparison of different methods of determination of the thresholds for fatigue crack propagation. In: Fatigue Thresholds, EMAS, Warley, pp. 45-57.

Hertzberg, R, Herman, W.A., Clark, T. and Jaccard, R., 1992. Simulation of short crack and other low closure loading conditions utilizing constant  $K_{max} \Delta K$  –decreasing fatigue crack growth procedure. In Larsen, J. M. and Allison, J. E. (Eds.), Small-crack test methods, ASTM STP 1149, ASTM, West Conshohocken, pp. 197-220.

JSME, 2000. JSME S NA1-2000 Fitness-for-service code for nuclear power plants. JSME, Tokyo.

Lang, M., Hartman, G. A., and Larsen, J. M., 1998. Investigation of an abnormality in fatigue crack growth curves – the Marci effect. Scripta Materialia. 38, 1803-1810.

Marci G., 1996. Failure mode below 390 K with IMI 834, In Lütjering, G. and Newack, H. (Eds.), Proceedings of the Sixth International Fatigue Conference, Vol. 1, Pergamon, Oxford, pp. 493-498.

Newman, J. A., Riddell, W. T. and Piascik, R. S., 2000. Effect of  $K_{max}$  on fatigue crack growth

T. Meshii, et al., Nuclear Engineering and Design, Vol. 220, No. 3, pp. 285-292 (2003. 2).

threshold in aluminum alloys, In Newman, J. C. and Piascik, R. S. (Eds), Fatigue crack growth thresholds, endurance limits and design, ASTM STP 1342, ASTM, West Conshohocken, pp. 63-77.

Paris, P. C. and Erdogan, F., 1963. A critical analysis of crack propagation laws. Trans. ASME, Ser.D. 85, 528-534.

#### Acknowledgements

Part of this research was supported by a grant from the Japan Nuclear Cycle Development Institute.

List of figures and tables

Fig. 1 Testing system

Fig.2 Geometry of CT test specimen

Fig. 3 Comparison of planned and measured  $\Delta K$  in the test (SUS304,  $K_{\max} = 31 \text{ MPam}^{1/2}$ )

Fig. 4 Test results (HT60)

Fig. 5 Test results (SS400)

Fig. 6 Test results (SUS304)

Fig. 7 Test results (S55C)

Fig. 8 Comparison of test results with the JSME code (carbon steel)

Fig. 9 Comparison of test results with the JSME code (stainless steel)

Fig. 10 Striation-like marks found in the Paris region (S55C,  $K_{\max} = 50 \text{ MPam}^{1/2}$ ,  $da/dN \approx 1 \times 10^{-5}$  mm/cycle)

Fig. 11 River pattern found in the near threshold region (S55C,  $K_{\max} = 50 \text{ MPam}^{1/2}$ ,  $da/dN \approx 1 \times 10^{-7}$  mm/cycle)

Table 1 Chemical composition of test specimens

Table 2 Mechanical properties of test specimens

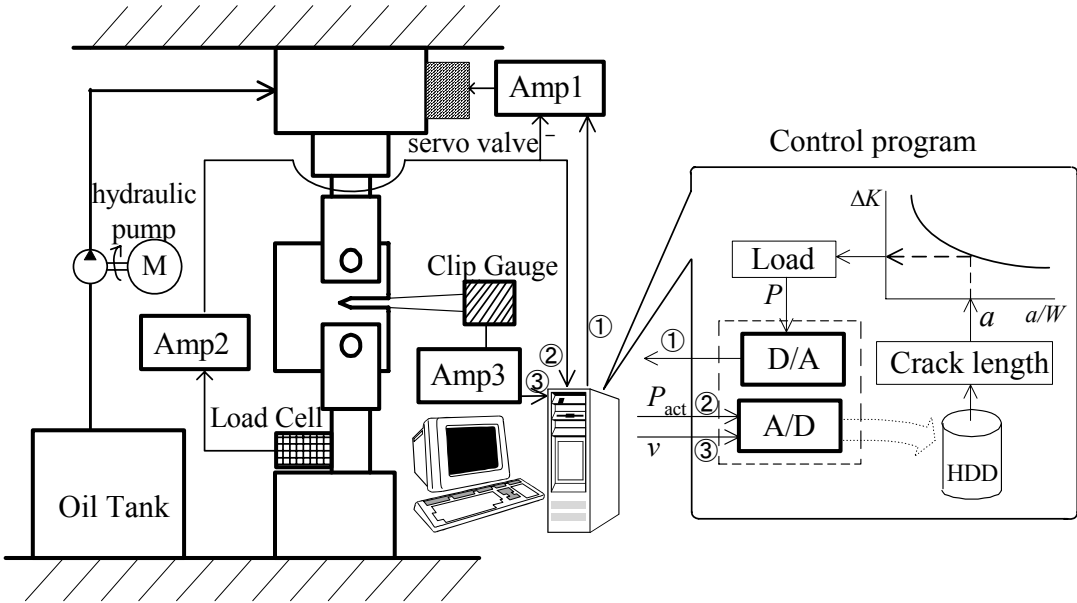


Fig. 1 Testing system

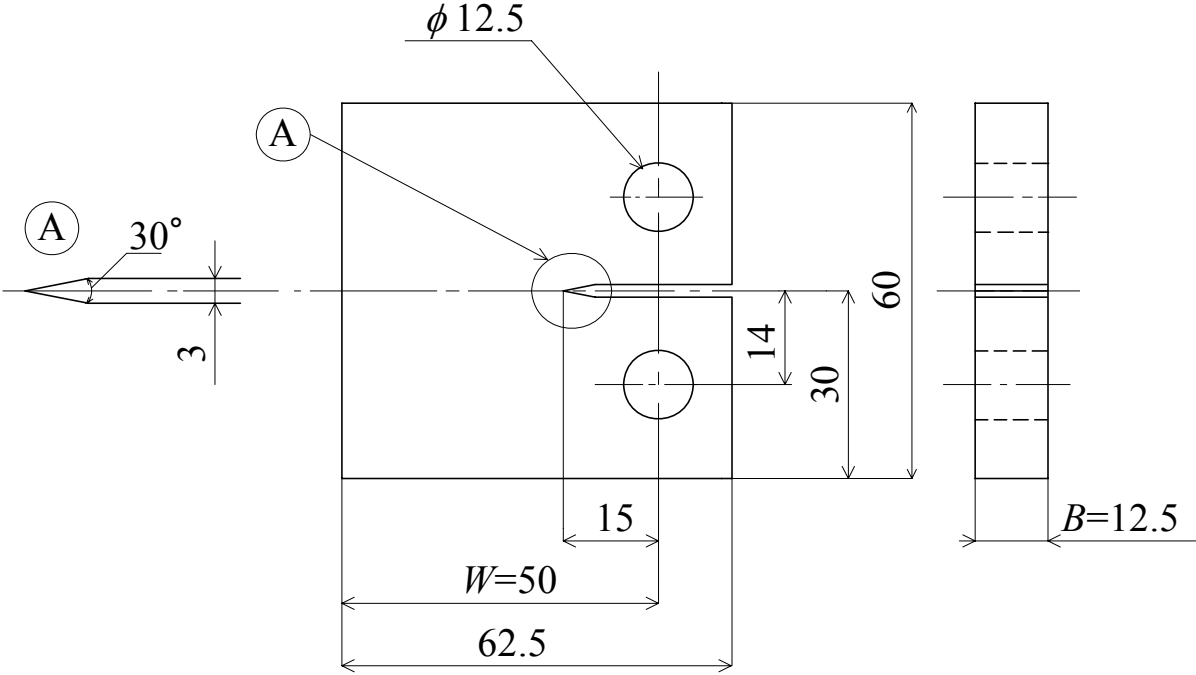


Fig.2 Geometry of CT test specimen

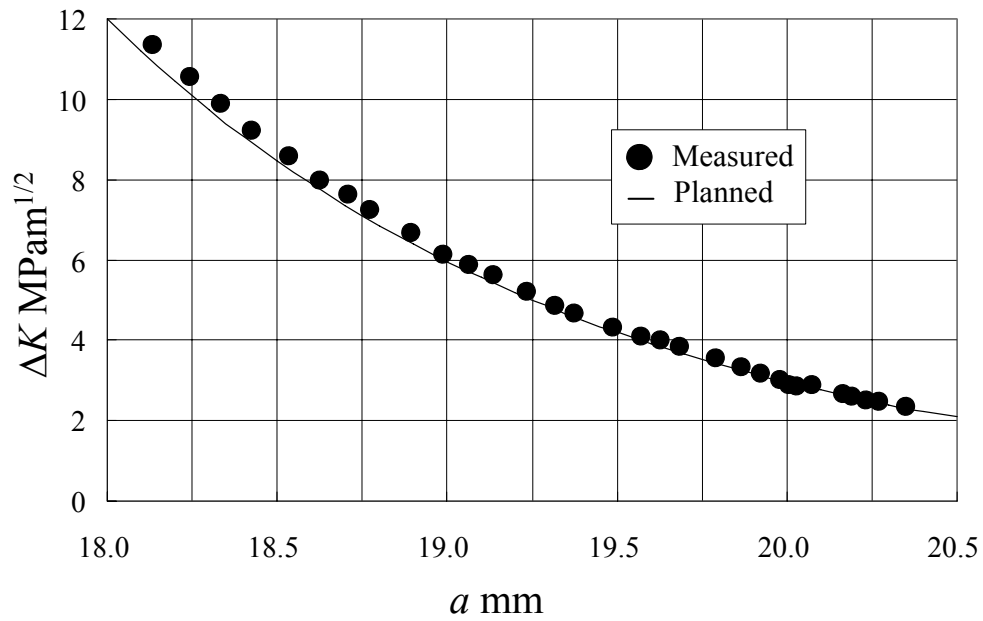


Fig. 3 Comparison of planned and measured  $\Delta K$  in the test (SUS304,  $K_{\max} = 31 \text{ MPam}^{1/2}$ )

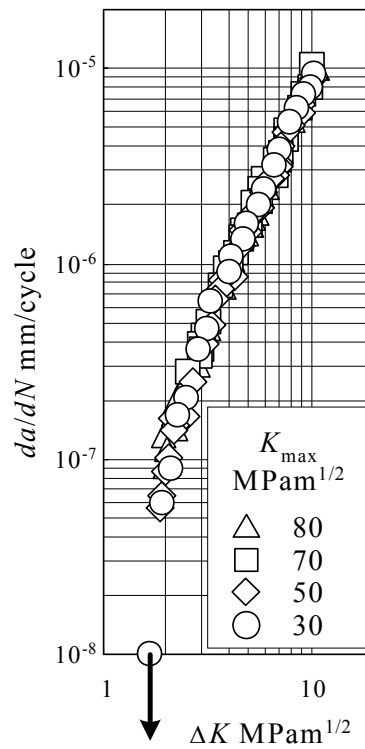


Fig. 4 Test results (HT60)

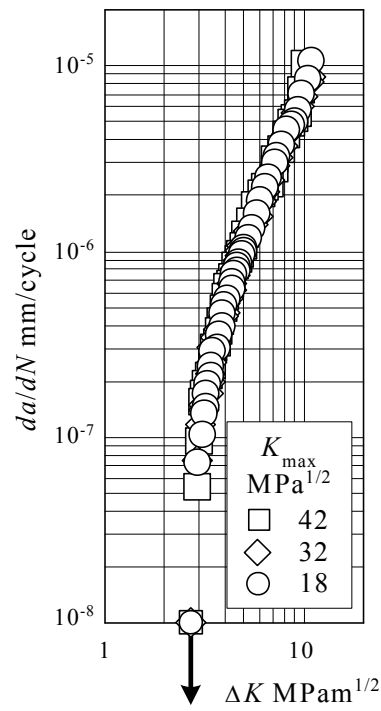


Fig. 5 Test results (SS400)

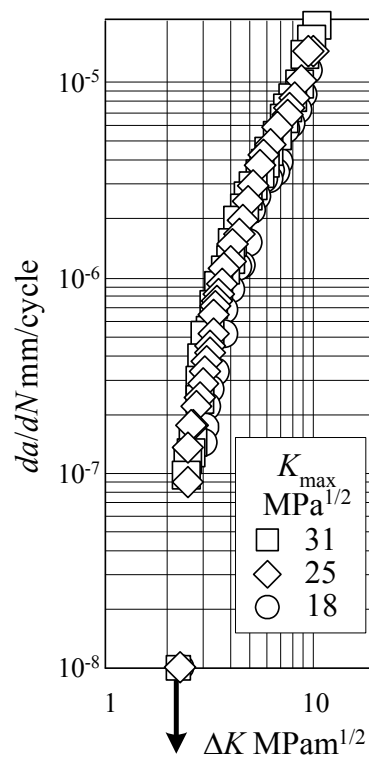


Fig. 6 Test results (SUS304)

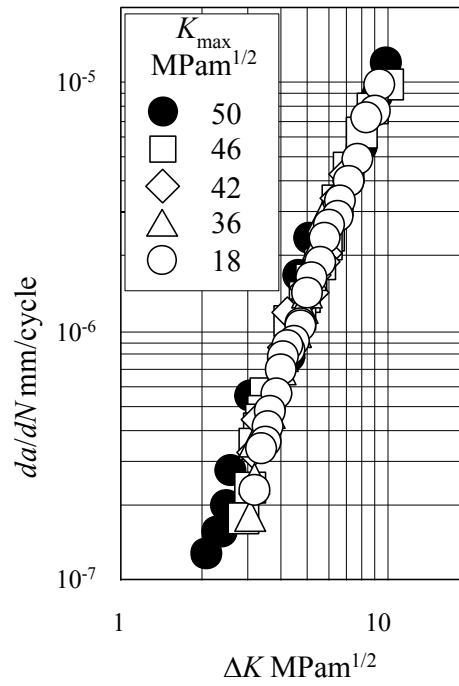


Fig. 7 Test results (S55C)

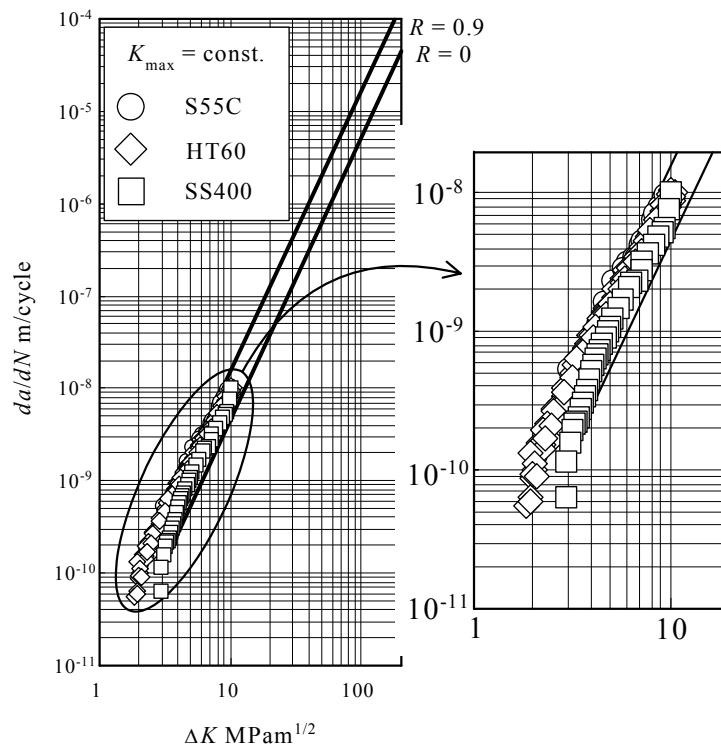


Fig. 8 Comparison of test results with the JSME code (carbon steel)

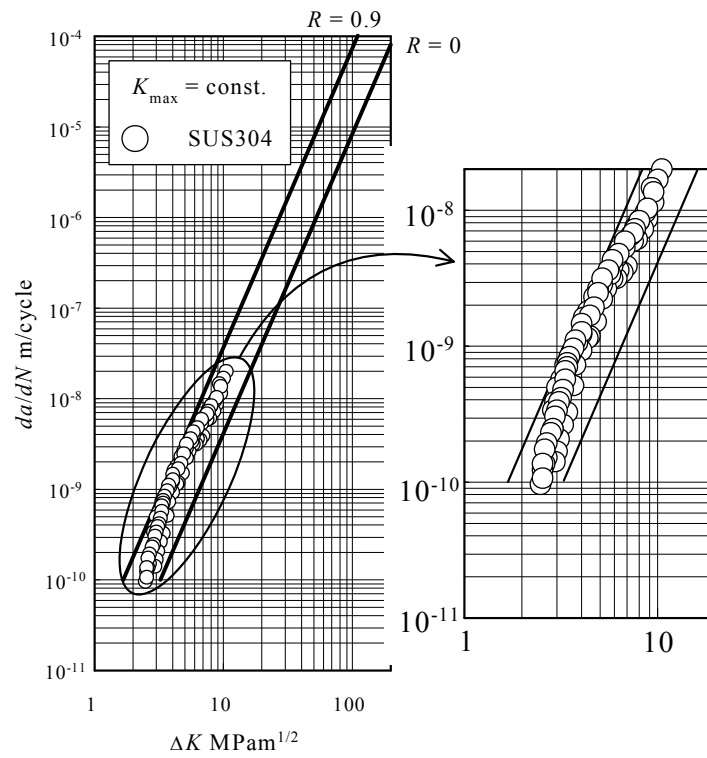


Fig. 9 Comparison of test results with the JSME code (stainless steel)

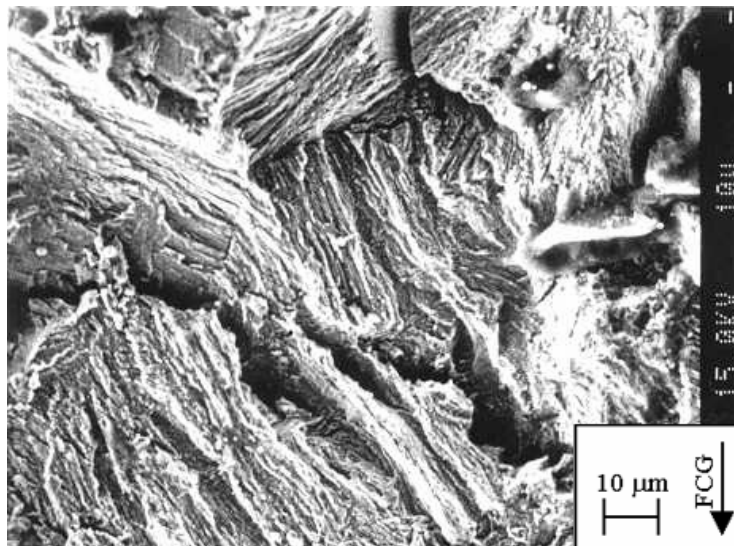


Fig. 10 Striation-like marks found in the Paris region

(S55C,  $K_{\max} = 50 \text{ MPam}^{1/2}$ ,  $da/dN \approx 1 \times 10^{-5} \text{ mm/cycle}$ )

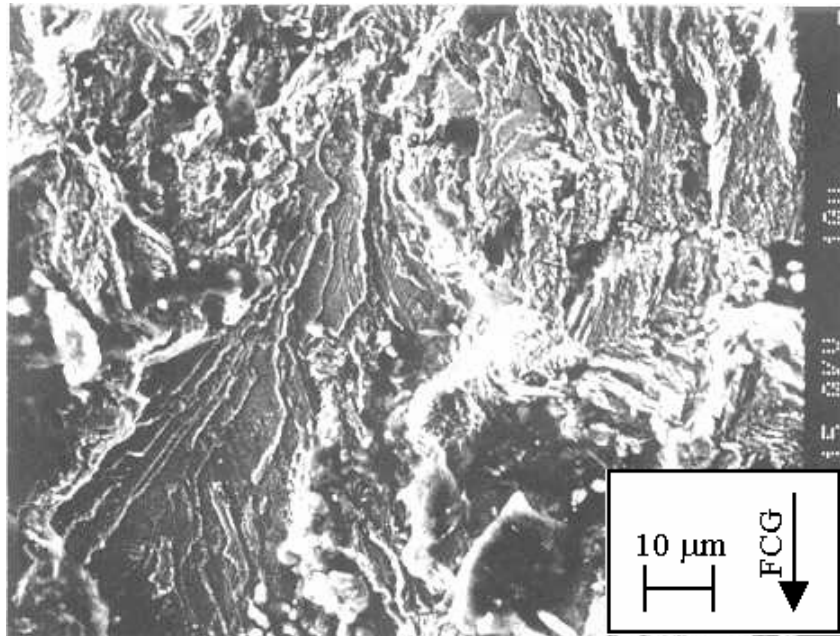


Fig. 11 River pattern found in the near threshold region

(S55C,  $K_{\max} = 50 \text{ MPam}^{1/2}$ ,  $da/dN \approx 1 \times 10^{-7} \text{ mm/cycle}$ )

Table 1 Chemical composition of test specimens

	C	Si	Mn	P	S	Cu	Ni	Cr	Nb	B	Fe
S55C	0.53	0.20	0.66	0.007	0.003	0.01	0.02	0.02	-	-	Bal.
HT60	0.12	0.25	1.45	0.008	0.003	0.01	0.02	0.03	0.02	0.0001	Bal.
SS400	0.12	0.22	0.58	0.021	0.017	-	-	-	-	-	Bal.
SUS304	0.05	0.59	1.02	0.028	0.008	-	9.11	18.35	-	0.0001	Bal.

Table 2 Mechanical properties of test specimens

	Yield Point	Tensile Strength
	MPa	MPa
S55C	375	724
HT60	520	631
SS400	275	438
SUS304	225	608